

ORIGINAL RESEARCH PAPER

## Green Route Synthesis of Manganese Oxide Nanoparticles by Using Methanolic Extract of *Sapindus mukorossi* (reetha)

Geetanjali\*, Anshu Tamta, Bhuwan Chandra, Narain Datt Kandpal, Rajendra Joshi

Department of Chemistry, Kumaun University, S. S. J. Campus Almora, 263601, Uttarakhand India

Received: 2023-12-22

Accepted: 2024-03-15

Published: 2024-05-12

### ABSTRACT

Nanoparticles of manganese oxide have been synthesized by a green chemistry approach using manganese chloride ( $MnCl_2 \cdot 2H_2O$ ), potassium permanganate ( $KMnO_4$ ), and methanolic extract of *Sapindus mukorossi* (reetha). In this study, we report here a simple ecofriendly green route to synthesize  $MnO_2$  nanoparticles. Manganese oxide nanoparticles were characterized by Fourier Transform Infra-Red (FTIR), UV-Vis spectral analysis, High-Resolution Transmission Electron Microscope (HRTEM), and Scanning Electron Microscope (SEM). The surface morphology showed that the  $MnO_2$  nanoparticles were uniformly dispersed. The average particle size was found 16 nm obtained by X-ray Diffraction (XRD), analysis. To find particle size DLS analysis has been done. The thermal stability of the nanoparticles with the temperature increase has been determined by Thermo-gravimetric Analysis (TGA) measurement. The synthesized manganese oxide nanoparticles were screened for antibacterial activities on gram-positive bacteria *Staphylococcus aureus*, *Bacillus subtilis*, and gram-negative bacteria *Pseudomonas aeruginosa*, *Escherichia coli*. The results of the antibacterial study suggest that the manganese oxide nanoparticles can be useful for effective growth inhibitors in microorganisms with applications to medical devices and antimicrobial-controlled systems. The order of the reactivity towards the zone of inhibition of microorganisms observed in the order of *Escherichia coli* (9mm) > *Pseudomonas aeruginosa* (8.3mm) > *Bacillus subtilis* (7.3mm) > *Staphylococcus aureus* (5.3mm).

**Keywords:** Green chemistry approach,  $MnO_2$  nanoparticles, *Sapindus mukorossi*, Antibacterial activity

### How to cite this article

Geetanjali., Tamta A., Chandra B., Kandpal N. D., Joshi R., Green Route Synthesis of Manganese Oxide Nanoparticles by Using Methanolic Extract of *Sapindus mukorossi* (reetha). J. Water Environ. Nanotechnol., 2024; 9(2): 211-222. DOI: 10.22090/jwent.2024.02.07

### INTRODUCTION

Transition metal oxides have scientific and technological importance for the last decades due to their specific properties related to optical, catalytic, electric, and magnetic fields [1]. Metallic nanoparticles of various sizes and shapes find specific areas of application [2]. Manganese oxides are largely studied because of their abundant nature and are used as green catalysts in the field of catalysis. Recently various methods have been used for the synthesis of metal nanoparticles such as chemical reduction [3], sonochemical method [4], one-step solution method at room temperature

[5], electrochemical techniques [6], hydrothermal method [7], polyol method [8], microemulsion method [9] and nowadays green chemistry route [10]. The use of benign material like plant leaf extract [11], bacteria [12], fungi [13], and enzymes [14], in the synthesis of nanoparticles is more cost-effective, environmentally friendly, having biomedical application due to the use of non-toxic material [15].

Secondary metabolites called Sapindus are produced by a wide variety of plant species. *Sapindus mukorossi*, a member of the family Sapindaceae, is commonly known by several names such as soapnut, soapberry, washnut,

\* Corresponding Authors Email: [geetanjali148@gmail.com](mailto:geetanjali148@gmail.com)



This work is licensed under the Creative Commons Attribution 4.0 International License.

To view a copy of this license, visit <http://creativecommons.org/licenses/by/4.0/>.

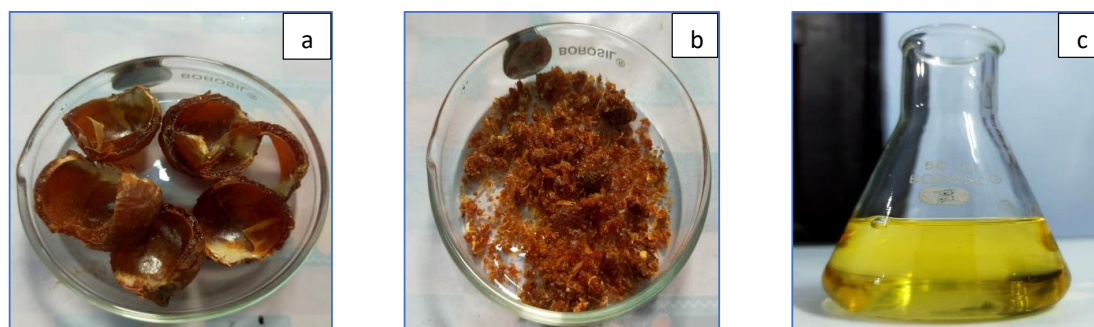


Fig. 1. Schematic representation of soapberry (a) soapberry fruits, (b) powdered extract of fruit pericarp, (c) methanolic extract of fruit pericarp of soapberry.

reetha, aritha, and dodan [16]. *Sapindus mukorossi* possesses antibacterial activity, insecticidal activity, spermicidal activity, anti-cancer activity, anti-inflammatory activity, antiplatelet aggregation activity, molluscicidal activity, and fungicidal activity [17]. In recent years manganese dioxide nanoparticles achieved a high rate of interest in the research field of material science due to their extensive applications in various fields like catalysts, lithium-ion batteries, biological fields, medicinal drug delivery, sensor and imaging techniques, etc. [18]. Due to its non-toxic behavior, it is safe to use in laboratory reactions, products made from manganese are biocompatible and non-hazardous. Manganese oxide nanoparticles have attracted extensive attention in fundamental and potential technological applications in various fields. From various studies, it is well known that  $MnO_2$  has different crystal structures. As we concluded based on previous studies  $MnO_2$  nanoparticles are easy to prepare by using a wet chemical method for its synthesis and have great stability and durability [19].

As for the environmental approach, plant extracts using reduction methods can be considered as more effective green approaches for synthesizing metal oxide nanoparticles. Green synthesis of metal oxides can be performed under mild conditions such as low temperature or at room temperature [20]. Recent reports on the use of *Sapindus mukorossi* extracts in the synthesis of other metal nanoparticles have motivated us to synthesize manganese dioxide nanoparticles using *Sapindus mukorossi*.  $MnO_2$ , due to its significant electrochemical performance, limited environmental toxicity, and lower production cost, has extensive applications in energy storage devices [21]. It is known that the phases, sizes,

and morphologies of nanomaterials have a great influence on their properties and applications; therefore, many research efforts have focused on rational control of the phase, shape, size, and dimensionality of nanomaterials [22]. In the present study, we have focused on the synthesis of manganese oxide nanoparticles and its characterization has been done by analytical instrumentation, along with SEM, TEM, XRD, FT-IR, TGA, and UV-Vis, DLS. The biologically synthesized nanoparticles were achieved by antibacterial activity against selected organisms using *S. aureus* (+ve), *B. subtilis* (+ve), *P. aeruginosa* (-ve), and *E. coli* (-ve). The metal oxide nanoparticles of manganese oxide (IV) have been tested against gram-positive and two gram-negative bacteria.

## MATERIALS AND METHODS

Every chemical and solvent that was used came from the analytical reagent grade Merck (India) Ltd and all the samples were prepared by using fresh double-distilled water. In a typical synthesis, Potassium permanganate ( $KMnO_4$ ), double distilled water, manganese (II) chloride, and methanolic extract of *Sapindus mukorossi* have been utilized to synthesize  $MnO_2$  nanoparticles in a round bottom flask, under constant magnetic stirring. After that, the product was filtered, washed, and dried for further characterization.

### Plant material collection and extraction:

The fruits of *Sapindus mukorossi* were collected from Bhatronjkhana Ranikhet district Almora Uttarakhand, directly from the natural trees. The collected fruits were washed thrice with distilled water and dried in sunlight. The peel of the fruits was separated from the seeds by cutting the whole fruit. The peel portion was used for the extraction of plant surfactant. The peel material was crushed

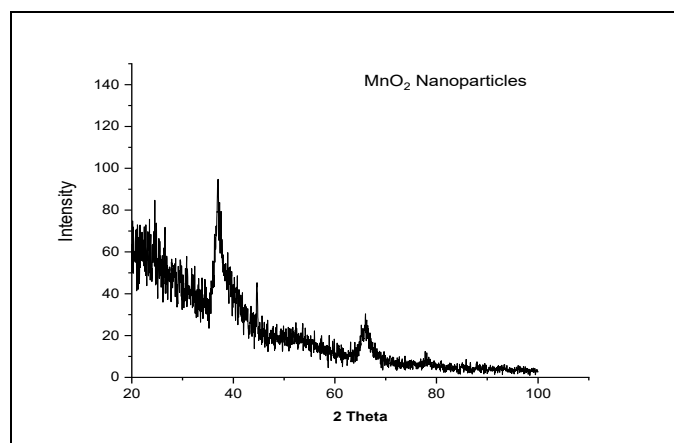


Fig. 2. XRD pattern of  $\text{MnO}_2$  nanoparticles synthesized with *Sapindus mukorossi*.

in a grinder and then in a mortar to prepare the small particle size. The crushed material of peels was 12.5 gr in 250 mL of methanol and was kept for seven days at room temperature. Finally, the content was heated up to 35 °C and an extract of the surfactant was collected by centrifuge with the speed of 3700 rpm (medico centrifuge). The extract obtained has a light yellow color which was used in the present study and mentioned in Fig. 1. The extract was collected in a clean and dried container and it was stored for further uses.

#### Synthesis of manganese dioxide nanoparticles

Synthesis of manganese dioxide nanoparticles was performed by using the sol-gel method. The method was performed by using manganese (II) chloride of (3.76 gr), in 100 mL of double distilled water containing methanolic extract of *Sapindus mukorossi* which was dissolved in 100 mL aqueous solution of potassium permanganate (4.76 gr), under continuous magnetic stirring at room temperature for 1 hour. The resulting black precipitate was filtered and washed with ethanol and double distilled water and kept in the air for 24 hours. The powdered black precipitate of  $\text{MnO}_2$  nanoparticle was dried at 80 °C for 15 hours.

#### Characterization of $\text{MnO}_2$ nanoparticle

In our studies, the  $\text{MnO}_2$  nanoparticles were synthesized and characterized by XRD (PW3050/60 X-ray diffractometer), UV-Vis spectroscopy ( $\lambda = 750$  (Perkin Elmer) UV-Vis NIR Spectrophotometer), FTIR (FT-IR Spectrum 2 Perkin Elmer), TGA (STA 6000 (Perkin Elmer), SEM (Carl Zeiss EVO 40 used at 20 KV (Cambridge

UK), HRTEM (HRTEM, Tecnai G2 20 S-TWIN [FEI], 200 kV) have been obtained to confirm the nano size of the materials. Powder XRD analysis has been carried out to examine the crystallinity and to check the purity. The optical properties of the nanoparticle were analyzed using UV-Vis spectroscopy. The presence of chemical bonds was analyzed by FTIR spectroscopy. The thermal stability of the synthesized nanoparticle was analyzed by TGA. Particle size and Morphology of the synthesized manganese dioxide nanoparticles were analyzed using HRTEM, antibacterial activity test against *S. aureus*, *B. subtilis*, *P. aeruginosa*, and *E. coli* by zone inhibition method. For antibacterial activity, Bacterial Culture (*S. aureus*, MTCC96 *B. subtilis* MTCC 1133, *P. aeruginosa* MTCC3541, *E. coli* MTCC- 452), Mueller-Hilton Agar (MHA-SRL Chem-24756) Plates have been utilized. To detect particle size DLS analysis has been done in (LENOVO Litesizer 500 in an advanced cumulent model).

## RESULTS AND DISCUSSION

The chemical synthesis of manganese dioxide nanoparticles shows different characterization patterns like XRD, UV-Vis spectrum, TGA, FTIR, HRTEM, SEM, DLS, and antibacterial activity. All the characterized data is discussed below.

#### X-Ray Diffraction Analysis

The phase and purity of the products are examined by X-ray diffraction (XRD), from the XRD pattern it is clear that manganese dioxide metal nanoparticles synthesized were purely crystalline. X-ray diffraction (XRD) analysis was

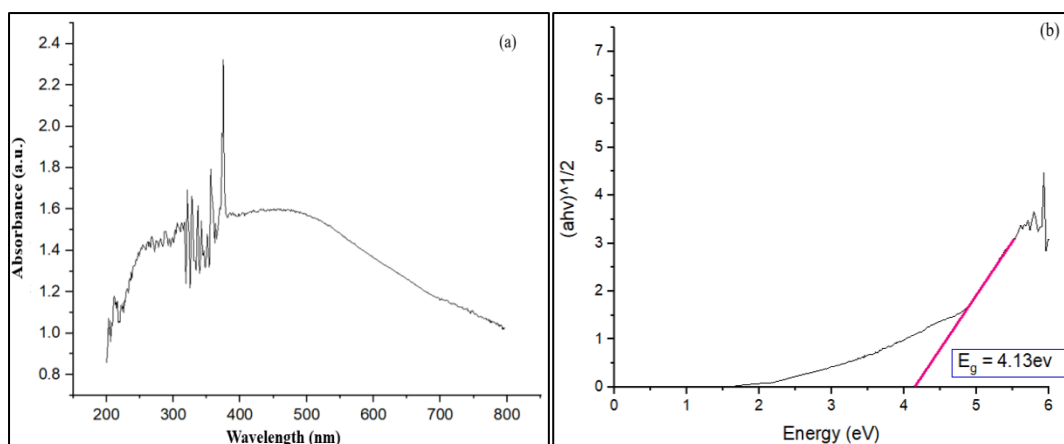


Fig. 3. (a) UV-Vis spectrum of  $\text{MnO}_2$  nanoparticle (b) Energy band gap of  $\text{MnO}_2$  nanoparticle synthesized with *Sapindus mukorossi*.

carried out in powder form and typical diffraction patterns are shown in Fig. 2. The intensity of the peaks indicates the crystallinity of the biologically synthesized nanoparticle [23]. The size of crystalline nanoparticles was calculated by using Debye-Scherrer equation, Where D is the mean size of the crystal,  $\lambda$  denotes the wavelength of the incident x-ray,  $\beta$  is full-width half maxima, and  $\theta$  is Bragg's angle. The particle size of the nanoparticle was estimated to be 8 nm and 24 nm and the average particle size was approximately 16 nm [24].

#### UV-Vis Spectroscopy

UV-visible absorption study is one of the most convenient techniques for characterizing nanoparticles and thus provides information about the optical properties of nanoparticles [25]. The electronic absorption spectrum of synthesized  $\text{MnO}_2$  nanoparticles showed absorption maxima ( $\lambda_{\text{max}}$ ) at 380 nm which indicated the formation of  $\text{MnO}_2$  nanoparticles [26]. UV-Vis provides high stability and accuracy performance. The UV-Vis absorption spectra were used to estimate optical band gaps [27], the optical band gap ( $E_g$ ) value is 4.13 eV with increasing the  $\text{MnO}_2$  percentage as can be seen in Fig. 3, (b). This can be attributed to the photoexcitation of electrons from the valence band to the conduction band [28].

#### FT-IR Analysis

FTIR spectroscopy is used to determine the presence of functional groups on the synthesized nanoparticles. In the FTIR spectra of manganese dioxide nanoparticles assisted with methanolic

extract of *Sapindus mukorossi* sample. The wave numbers of the maximum intensity in the spectra of manganese dioxide are measured from 400-4000 $\text{cm}^{-1}$ . The first peak at 530.99 $\text{cm}^{-1}$  reveals the presence of a metal-oxygen stretching vibration band of manganese in the oxide state and confirms the formation of manganese dioxide. The presence of a broad peak at 3430 $\text{cm}^{-1}$  corresponds to the vibrations of the alcoholic O-H group, another peak is obtained at 1059 $\text{cm}^{-1}$  due to the C=O stretching of carbinol. The absorption band near 1631 $\text{cm}^{-1}$  confirms the presence of carboxylic groups. The bands at 1222 and 1383 $\text{cm}^{-1}$  may be due to the hydrocarbon chain of soapnut assigned to C-O and C=C stretching [29]. The FTIR spectra observed in this study are consistent with reported literature [30]. It is important to mention here that during the synthesis of manganese oxide, we have synthesized the nanoparticles at low temperatures due to which the absorption of precursors at the surface of the particles has a significant influence in the spectra. The changes in the intensity or small shifts of the various spectral bands may be due to the interactions between the nanoparticles and their precursors. The bands at 2919  $\text{cm}^{-1}$  and 2850  $\text{cm}^{-1}$  can represent the absorption of a phenolic ring of saponin present in soapnut extract or C-H stretch of alkenes as reported in the literature [31]. The FTIR spectrum of the methanolic extract of *Sapindus mukorossi* was recorded to compare the FTIR spectrum of the  $\text{MnO}_2$  nanoparticle. The spectrum is shown in Figs. 4 (b) and (a). It is clear from Fig. 4 (a and b) that the presence of peaks in both the spectra at 3324  $\text{cm}^{-1}$  and 3430  $\text{cm}^{-1}$  are

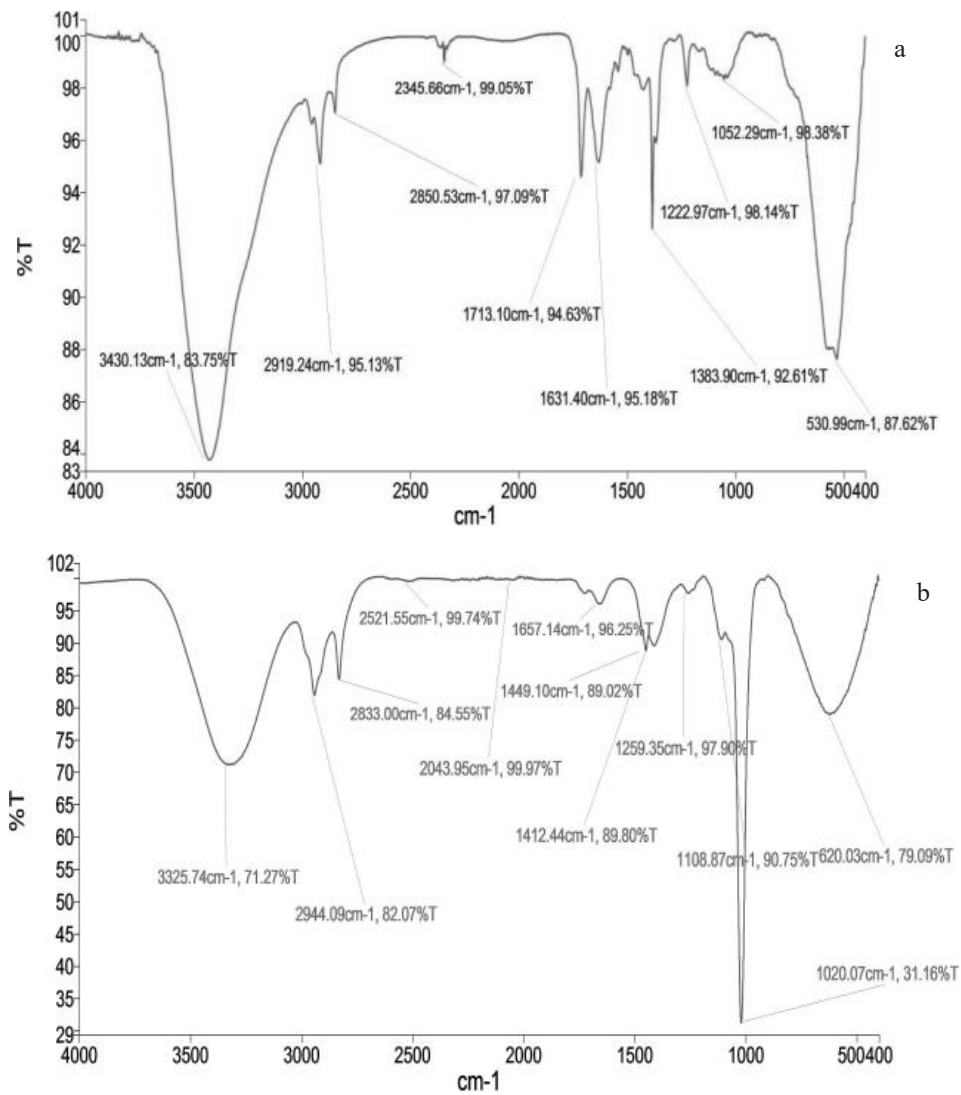


Fig. 4. (a) FT-IR spectrum Plot between wave number (cm<sup>-1</sup>) and transmittance (%) of MnO<sub>2</sub> nanoparticle synthesized with Sapindus mukorossi (b) FT-IR spectrum of methanolic extract of soapnut.

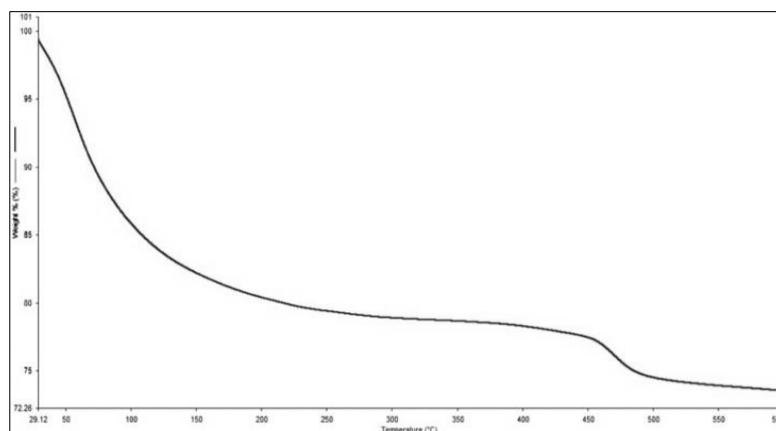


Fig. 5. TGA analysis of MnO<sub>2</sub> nanoparticle plot between temperature and weight % synthesized with Sapindus mukorossi.

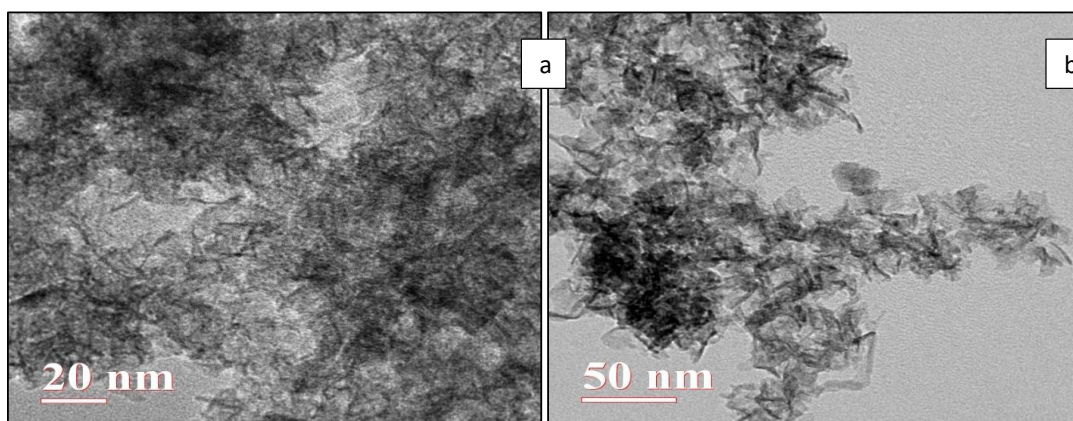


Fig. 6. TEM images of MnO<sub>2</sub> nanoparticle synthesized with *Sapindus mukorossi* (a) 20nm scale (b) 50nm scale.

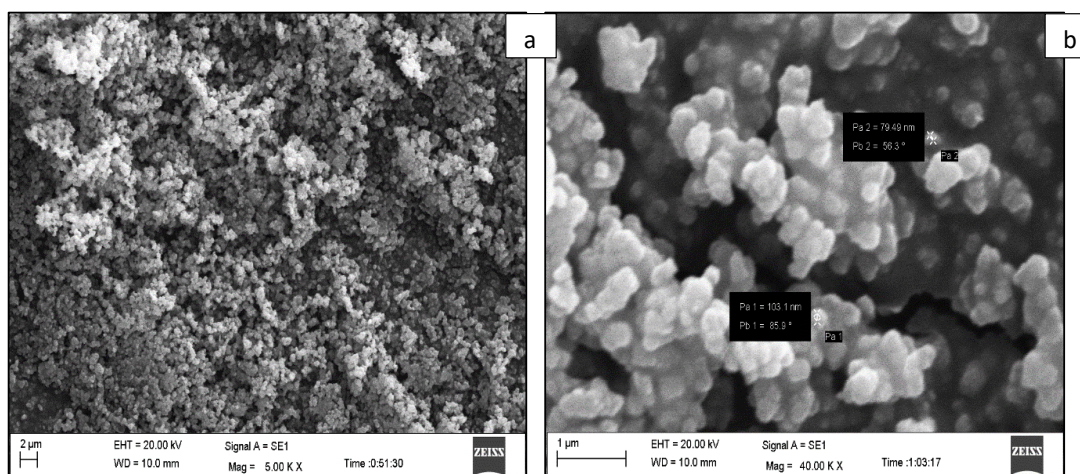


Fig. 7. SEM images of MnO<sub>2</sub> nanoparticle synthesized with *Sapindus mukorossi* (a) 2μm (b) 1μm.

in the same region which is the characteristic of O-H alcoholic stretch and H-bonding of water molecules. The peaks at 1119 cm<sup>-1</sup>, 1417 cm<sup>-1</sup> and 1222 cm<sup>-1</sup> are the C-C stretch in aromatic rings whereas 620 cm<sup>-1</sup> represents the presence of N-H amine group which confirms the metal oxide characteristics bond at 530 cm<sup>-1</sup> in the case of nanoparticle spectra.

#### TGA Analysis

TGA analysis was used to demonstrate the thermal stability of the synthesized nanoparticles. The analysis was carried out in the range of 30-600 °C [32]. The data shows the reduction in the weight percentage of the nanoparticle with an increase in the temperature, which is attributed to the decomposition of water molecules present on the surface of the nanoparticles [33]. It is

visible from Fig. 5 that the nanoparticle favors the thermal gravimetric analysis by its decreasing weight percent. In this study, stable nanoparticles of MnO<sub>2</sub> were produced by using the *Sapindus mukorossi* at room temperature. The thermal stability of MnO<sub>2</sub> nanoparticles was accomplished by thermal gravimetric and differential thermal analysis from 30 to 600 °C temperature and weight percentage from 72.16 to 100% which shows the TGA behavior of MnO<sub>2</sub> nanoparticles.

#### HRTEM Analysis

HRTEM image gives detailed information about the interior structural characteristics of as-prepared MnO<sub>2</sub> nanoparticles. HRTEM images give a clear shape and size of the nanoparticle. It is clear from HRTEM images that the nanoparticles are grown in needle shape. In the TEM image

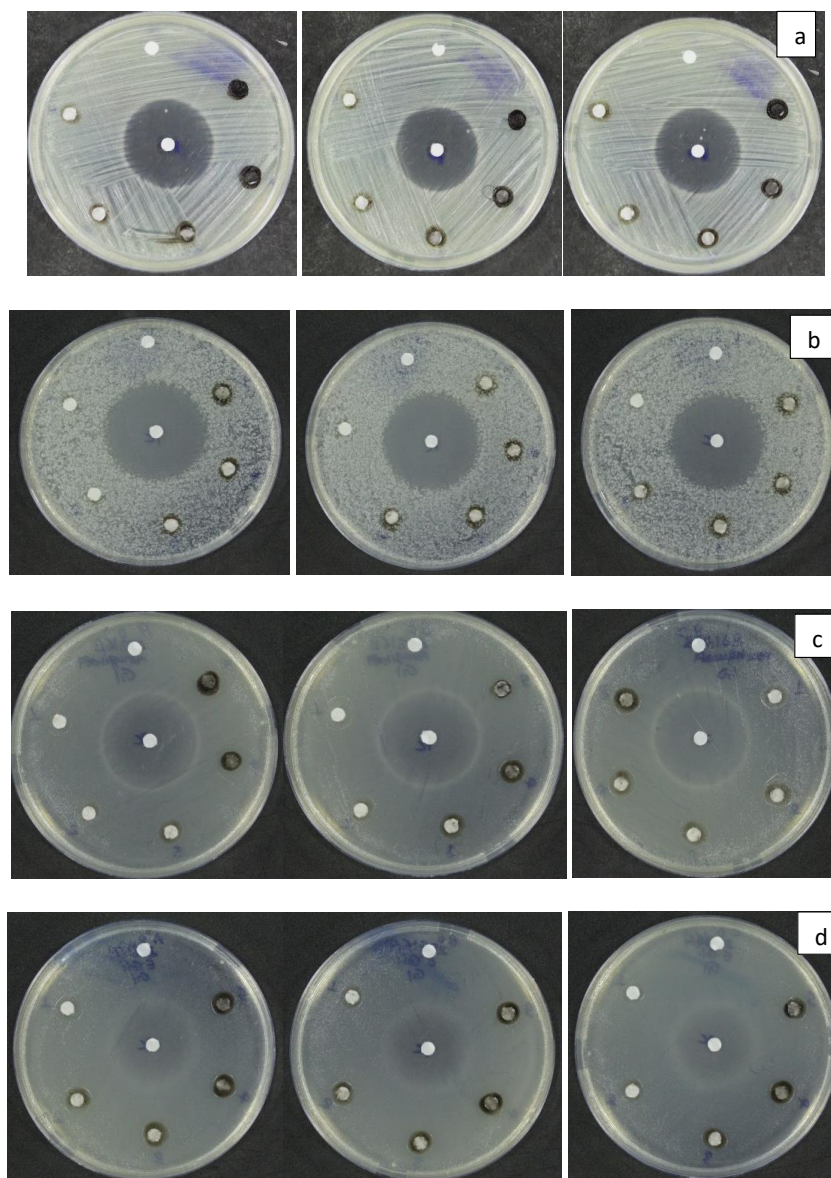


Fig. 8. The plates of (a) *S. aureus*, (b) *B. subtilis*, (c) *P. aeruginosa*, (d) *E. coli* showing bacterial culture of  $MnO_2$  nanoparticle synthesized with *Sapindus mukorossi* by following Zone Inhibition Method through disc diffusion method.

shown in Fig. 6, the crystalline shape of the particle/crystals is more distinguished the scale used is also large 50nm. From this figure, the needle-to-needle distance was calculated for eight samples. The average of the eight data is 14.953, 11.983, 15.285, 10.986, 16.213, 3.963, and 5.151 the average size of the particle obtained from the data was 10.7 nm which is justified with the size calculated from the XRD spectra 8.0 nm in the experimental limit. TEM images have been observed extremely small in size [34].

#### SEM Analysis

SEM technique was used to examine the surface morphology of the manganese oxide nanoparticles. The image represented in Fig. 7, shows the irregular spherical shape due to their external small dimension and high surface energy [35]. It is well acknowledged that surface morphology has an important impact on the performance of nanostructure materials. SEM micrograph reveals the overall appearance of the combustion-derived product [36]. SEM morphology of  $MnO_2$  nano-crystalline particles

Table 1. Antibacterial activity of MnO<sub>2</sub> nanoparticles against *S. aureus*, *B. subtilis*, *P. aeruginosa*, and *E. coli* showing maximum zone inhibition under different concentrations.

S. No.	Microorganism	Max. ZI (mm)	conc. (µg)	PC (conc. in µg)
1.	<i>S. aureus</i>	5.3mm	50 µg	50 µg
2.	<i>B. subtilis</i>	7.3mm	50 µg	10 µg
3.	<i>P. aeruginosa</i>	8.3mm	50 µg	50 µg
4.	<i>E. coli</i>	9mm	250 µg	10 µg

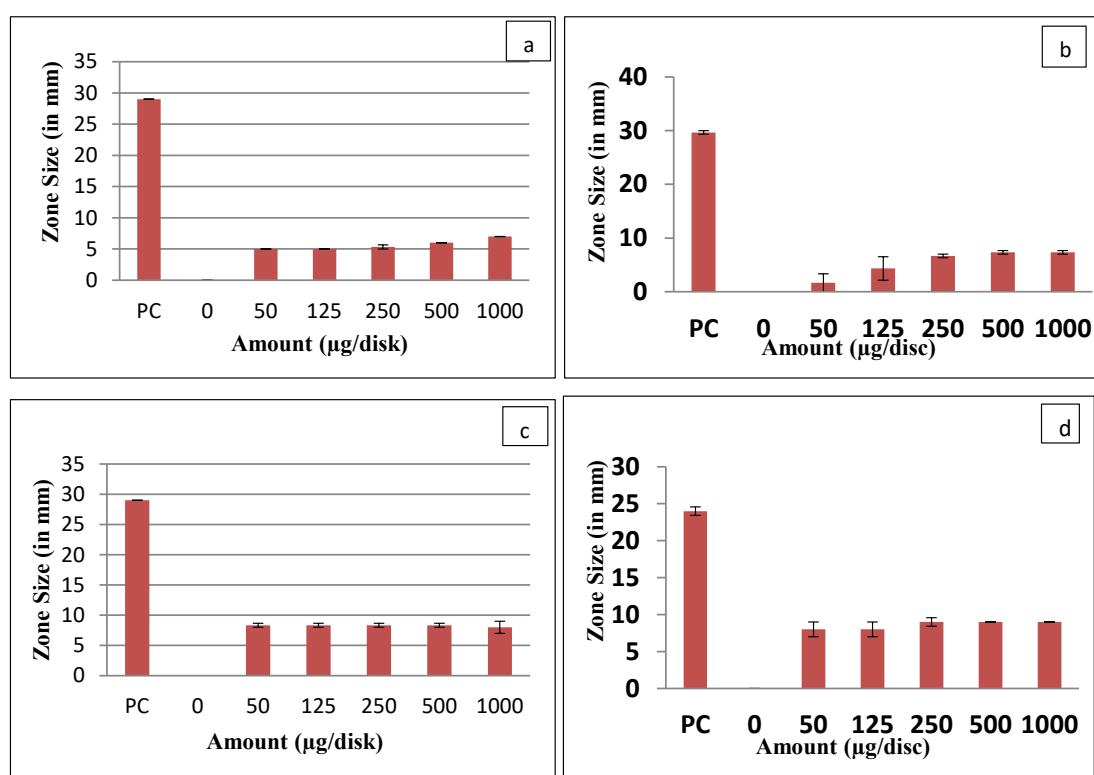


Fig. 9. Graphical representation of antibacterial activity for MnO<sub>2</sub> nanoparticle synthesized with Sapindus mukorossi against (a) *S. aureus*, (b) *B. subtilis*, (c) *P. aeruginosa*, (d) *E. coli*, between zone size (in mm) and amount (µg/disc).

found to have an irregular spherical shape, harshly agglomerated, and aggregated between the observed particles. The SEM pictures of prepared MnO<sub>2</sub> nanoparticles at different diameters, at 2 µm and 1 µm were supported with the previously published data [37]. The MnO<sub>2</sub> nanoparticles consist of separated nanostructures, due to the activation of the surface of nanoparticles, some areas have been ruptured and also show small cubic-shaped nanoparticles [38]

#### Antibacterial activity

The Antibacterial activity was checked by following the Zone Inhibition Method (Kirby-Bauer method). The MHA plates were inoculated by spreading with 100 µl of Bacterial culture, *S. aureus*, *B. subtilis*, *P. aeruginosa*, and *E. coli* (adjusted to 0.5 McFarland Unit - approx cell density (1.5 X 10<sup>8</sup> CFU/mL) and followed by placing the discs containing 10 µl of different

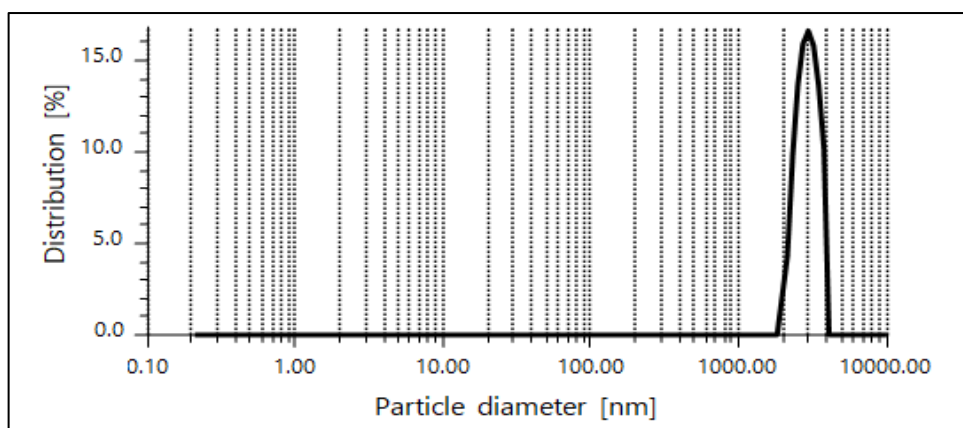


Fig. 10. DLS of MnO<sub>2</sub> nanoparticle synthesized with Sapindus mukorossi showing particle size distribution intensity.

Table. 2. Representation of DLS measured hydrodynamic diameter of MnO<sub>2</sub> nanoparticles synthesized with Sapindus mukorossi. \_

Hydrodynamic diameter	4762 nm	Mean intensity	264.0 kcounts/s
Polydispersity index	54.9 %	Absolute intensity	337996.9 kcounts/s
Diffusion coefficient	0.1 μm <sup>2</sup> /s	Intercept g1 <sup>2</sup>	0.6097
Transmittance	2.1%	baseline	1.062

concentration (0 to 100 mg/ml). 10 % of the sample was taken and serially diluted to achieve the required amount to be loaded on the disc. One disc in each plate was loaded with solvent alone which served as vehicle control (Dimethyl Sulfoxide, SRL Chem- 28580) and Ciprofloxacin disc (10μg) (SRL Chem-78079), 2mg/ml was taken as a positive control. The plates of *S. aureus*, *B. subtilis*, *P. aeruginosa*, and *E. coli* were incubated (Basil Scientific Corp. India) at 37 °C for 24 hours. Clear zones created around the disc were measured and recorded.

Based on the results obtained from the study, when the test organism was treated with different amounts of sample on an agar plate, it was found that MnO<sub>2</sub> nanoparticles achieved the maximum zone of inhibition (ZI) estimated as mentioned in Table 1. having antibacterial activity against the test organisms *S. aureus*, *B. subtilis*, *P. aeruginosa*, and *E. coli* as compared to positive control. The zone of inhibition is an area around a disc on an agar plate where no bacterial growth is observed due to the presence of an antimicrobial agent. It is used to determine whether a particular

test organism is susceptible to the action of a particular antimicrobial agent or not.

We also looked at the broad-spectrum antibacterial activity of MnO<sub>2</sub> nanosheets and their ability to inhibit *S. aureus*, *B. subtilis*, *P. aeruginosa*, and *E. coli* by the surface plate assay a significant dose-dependent inhibitory effect was observed after exposure of different concentrations of MnO<sub>2</sub> nanoparticles. Different concentration of MnO<sub>2</sub> nano-sheet shows higher inhibitory effects on *S. aureus*, *B. subtilis*, *P. aeruginosa*, and *E. coli*, and the inhibition rate was higher to control the antimicrobial growth. These results indicated that MnO<sub>2</sub> nano-sheets have antibacterial activity against Gram-positive bacteria and Gram-negative bacteria [39].

#### DLS Analysis

To confirm the size of the MnO<sub>2</sub> nanoparticle synthesized using methanolic extract of the soapnut dynamic light scattering (DLS) analysis was conducted to calculate the particle size. Table 2 shows the the hydrodynamic particle sizes of MnO<sub>2</sub> nanoparticles that were analyzed to

detect the Brownian motion of particles, which is correlated to the particle size [40]. Based on the DLS analysis the results revealed that the size of the MnO<sub>2</sub> nanoparticle which is in agreement with the size obtained from XRD 8.0 nm there is only a variation of percent in results obtained from DLS and XRD (Fig. 10). The size of the nanoparticle obtained in our study is seven times smaller than the size obtained in using Tridax procumbers [41].

## CONCLUSION

Green synthesis of nanoparticles has a significant role in the field of nanotechnologies due to its non-toxic and environmentally friendly nature, the green route synthesis of nanoparticles is a significant step in the field of nano-chemistry. There is a massive difference between classical synthesis and green synthesis due to its cost-effectiveness and feasibility. MnO<sub>2</sub> nanoparticles have been successfully synthesized by using an eco-friendly method followed by a green synthesis route at room temperature in the aqueous medium of methanolic extract obtained from *Sapindus mukorossi* (soapnut). The synthesized manganese oxide nanoparticles have an extremely small size 8 nm which has potent antibacterial activity against *S. aureus*, *B. subtilis*, *P. aeruginosa*, and *E. coli*. The study is a primary step towards the application of antibacterial agents against other microorganisms.

## ACKNOWLEDGEMENT

The authors are thankful to their management and UGC-CSIR for the financial support and to MNIT MRC Jaipur, Rajasthan, India for providing analytical instrumentation facilities. For antibacterial activity analysis, we are thankful to Aakaar Biotechnologies Private Limited Lucknow, India. For DLS analysis we are thankful to SAIF Chandigarh Panjab University India. For SEM analysis we are thankful to Advanced Instrumentation Research Facility JNU New Delhi, India. The authors are thankful to Prof. Raj N. Mehrotra, former Professor and head of the Chemistry department at Jodhpur University for his valuable suggestions.

## CONFLICT OF INTEREST

The authors hereby declare that there is no conflict of interest.

## REFERENCES

- Ahmed, S.; Chaudhry, S. A.; Ikram, S., A review on biogenic synthesis of ZnO nanoparticles using plant extracts and microbes: a prospect towards green chemistry, *Journal of Photochemistry and Photobiology B: Biology*, 2017, 166, 272-284. <https://doi.org/10.1016/j.jphotobiol.2016.12.011>
- Seabra, A.B.; Haddad, P.; Duran, N., Biogenic synthesis of nanostructured iron compounds: applications and perspectives, *IET nanobiotechnology*, 2013, 7(3), 90-99. <https://doi.org/10.1049/iet-nbt.2012.0047>
- Narayanan, K.B.; Sakthivel, N., Green synthesis of biogenic metal nanoparticles by terrestrial and aquatic phototrophic and heterotrophic eukaryotes and biocompatible agents, *Advances in colloid and interface science*, 2011, 169(2), 59-79. <https://doi.org/10.1016/j.cis.2011.08.004>
- Majumdar, D.; Bhattacharya, S.K., Sonochemically synthesized hydroxy-functionalized graphene-MnO<sub>2</sub> nanocomposite for supercapacitor applications, *Journal of Applied Electrochemistry*, 2017, 47, 789-801. <https://doi.org/10.1007/s10800-017-1080-3>
- Arasu, M.V.; Arokiyaraj, S.; Viayaraghavan, P.; Kumar, T. S.; Duraipandiyar, V.; Al-Dhabi, N. A.; Kaviyarasu, K., One step green synthesis of larvicidal, and azo dye degrading antibacterial nanoparticles by response surface methodology, *Journal of Photochemistry and Photobiology B: Biology*, 2019, 190, 154-162. <https://doi.org/10.1016/j.jphotobiol.2018.11.020>
- Wang, H.Q.; Yang, G.F.; Li, Q.Y.; Zhong, X.X.; Wang, F.P.; Li, Z.S.; Li, Y.H., Porous nano-MnO<sub>2</sub>: large scale synthesis via a facile quick-redox procedure and application in a supercapacitor, *New Journal of Chemistry*, 2011, 35(2), 469-475. <https://doi.org/10.1039/C0NJ00712A>
- Hayashi, H.; Hakuta, Y., Hydrothermal synthesis of metal oxide nanoparticles in supercritical water, *Materials*, 2010, 3(7), 3794-3817. <https://doi.org/10.3390/ma3073794>
- Lu, C.Y.; Wey, M.Y.; Chen, L.L., Application of polyol process to prepare AC-supported nanocatalyst for VOC oxidation, *Applied Catalysis A: General*, 2007, 325(1), 163-174. <https://doi.org/10.1016/j.apcata.2007.03.030>
- Santra, S.; Tapeç, R.; Theodoropoulou, N.; Dobson, J.; Hebard, A.; Tan, W., Synthesis and characterization of silica-coated iron oxide nanoparticles in microemulsion: the effect of nonionic surfactants, *Langmuir*, 2001, 17(10), 2900-2906. <https://doi.org/10.1021/la0008636>
- Hussain, I.; Singh, N.B.; Singh, A.; Singh, H.; Singh, S.C., Green synthesis of nanoparticles and its potential application, *Biotechnology letters*, 2016, 38, 545-560. <https://doi.org/10.1007/s10529-015-2026-7>
- Zayed, M.F.; Eisa, W.H., Phoenix dactylifera L. Leaf extract phytosynthesized gold nanoparticles; controlled synthesis and catalytic activity, *Spectrochimica Acta Part A: Molecular and Biomolecular Spectroscopy*, 2014, 121, 238-244. <https://doi.org/10.1016/j.saa.2013.10.092>
- Hassani, S.M.; Nakhaei, M.M.; Forghanifard, M.M., Inhibitory effect of zinc oxide nanoparticles on *Pseudomonas aeruginosa* biofilm formation, *Nanomed. J*, 2015, 2, 121-128.
- Hameed, A.S.; Karthikeyan, C.; Ahamed, A.P.; Thajuddin, N.; Alharbi, N.S.; Alharbi, S.A.; Ravi, G., In



- vitro antibacterial activity of ZnO and Nd doped ZnO nanoparticles against ESBL producing Escherichia coli and Klebsiella pneumonia, Scientific reports, 2016, 6(1), 24312. <https://doi.org/10.1038/srep24312>
14. Asaikutti, A.; Bhavan, P.S.; Vimala, K.; Karthik, M.; Cheruparambath, P., Dietary supplementation of green synthesized manganese-oxide nanoparticles and its effect on growth performance, muscle composition and digestive enzyme activities of the giant freshwater prawn *Macrobrachium rosenbergii*, Journal of Trace Elements in Medicine and Biology, 2016, 35, 7-17. <https://doi.org/10.1016/j.jtemb.2016.01.005>
  15. Quester, K.; Avalos-Borja, M.; Castro-Longoria, E., Biosynthesis and microscopic study of metallic nanoparticles, Micron, 2013, 54, 1-27. <https://doi.org/10.1016/j.micron.2013.07.003>
  16. Chu, X.; Zhang, H., Catalytic decomposition of formaldehyde on nanometer manganese dioxide, Mod Appl Sci, 2009, 3(4), 177-182. <https://doi.org/10.5539/mas.v3n4p177>
  17. Mishra, S.; Thakur, M., Role of microwave assisted extraction for isolation of saponins from sapindus mukorossai and synthesis of its stable biofunctionalized silver nanoparticles and its hypolipidaemic activity, International Journal of Pharmaceutical Sciences and Research, 2016, 7(7), 2959.
  18. Singh, S.; & Ali, M., Sapindus mukorossi: a review article, J. Pharm. Innov, 2019, 8(12), 88-96.
  19. Dawadi, S.; Gupta, A.; Khatri, M.; Budhathoki, B.; Lamichhane, G.; Parajuli, N., Manganese dioxide nanoparticles: synthesis, application and challenges, Bulletin of Materials Science, 2020, 43, 1-10. <https://doi.org/10.1007/s12034-020-02247-8>
  20. Jayandran, M.; Haneefa, M, M.; Balasubramanian, V., Green synthesis and characterization of Manganese nanoparticles using natural plant extracts and its evaluation of antimicrobial activity, Journal of Applied Pharmaceutical Science, 2015, 5(12), 105-110. <https://doi.org/10.7324/JAPS.2015.501218>
  21. Prasad, K.S.; Patra, A., Green synthesis of MnO<sub>2</sub> nanorods using Phyllanthus amarus plant extract and their fluorescence studies, Green Processing and Synthesis, 2017, 6(6), 549-554. <https://doi.org/10.1515/gps-2016-0166>
  22. Rao, C.N.; Vivekchand, S.R.; Biswas, K.; Govindaraj, A., Synthesis of inorganic nanomaterials, Dalton Transactions, 2007, (34), 3728-3749. <https://doi.org/10.1039/b708342d>
  23. C. Kavitha.; S. Vinothini.; S. Barathi.; A. Sasi Kumar., Chemical Synthesis of Manganese Dioxide Nanoparticle by Using Co-Precipitation Method, International journal of innovative research in science, engineering and technology, 2020, 142-147.
  24. Jassal, V.; Shanker, U.; Gahlot, S.; Kaith, B. S.; Kamaluddin, Iqbal, M. A.; & Samuel, P., Sapindus mukorossi mediated green synthesis of some manganese oxide nanoparticles interaction with aromatic amines. Applied Physics A, 2016, (122), 1-12. <https://doi.org/10.1007/s00339-016-9777-4>
  25. Luo, Y., Preparation of MnO<sub>2</sub> nanoparticles by directly mixing potassium permanganate and polyelectrolyte aqueous solutions, Materials Letters, 2007, 61(8-9), 1893-1895. <https://doi.org/10.1016/j.matlet.2006.07.165>
  26. Joshi, N.C.; Joshi, E.; Singh, A., Biological Synthesis, Characterisations and Antimicrobial activities of manganese dioxide (MnO<sub>2</sub>) nanoparticles, Research Journal of Pharmacy and Technology, 2020, 13(1), 135-140. <https://doi.org/10.5958/0974-360X.2020.00027.X>
  27. Soldatova, A.V.; Balakrishnan, G.; Oyerinde, O.F.; Romano, C.A.; Tebo, B.M.; & Spiro, T.G., Biogenic and synthetic MnO<sub>2</sub> nanoparticles: size and growth probed with absorption and Raman spectroscopies and dynamic light scattering, Environmental science & technology, 2019, 53(8), 4185-4197. <https://doi.org/10.1021/acs.est.8b05806>
  28. Franchini, C.; Bayer, V.; Podloucky, R.; Paier, J.; & Kresse, G., Density functional theory study of MnO by a hybrid functional approach, Physical Review B, 2005, 72(4), 045-132. <https://doi.org/10.1103/PhysRevB.72.045132>
  29. Jaganyi, D.; Altaf, M.; & Wekesa, I., Synthesis and characterization of whisker-shaped MnO<sub>2</sub> nanostructure at room temperature, Applied Nanoscience, 2013, 3, 329-333. <https://doi.org/10.1007/s13204-012-0135-3>
  30. Yadav, V.; Shukla, R.; & Sharma, K.S., Impact of Zn-doped Manganese Oxide Nanoparticles on Structural and Optical Properties, Journal of Scientific Research, 2022, 14(3), 867-876. <https://doi.org/10.3329/jsr.v14i3.58542>
  31. Pooja, R.; Varsha, S. L.; Aliya, M. S.; Chetana Kumar, T.; Damini, B. M.; & Divya, H. K., Phytochemical screening, GCMS, UV-VIS and FTIR analysis of leaf methanolic extract of Sapindus mukorossi L, International Journal of Progressive Research in Science and Engineering, 2022, 3, 97-104.
  32. Schladt, T.D.; Graf, T.; Tremel, W., Synthesis and characterization of monodisperse manganese oxide nanoparticles-evaluation of the nucleation and growth mechanism, Chemistry of Materials, 2009, 21(14), 3183-3190. <https://doi.org/10.1021/cm900663t>
  33. Srivastava, V.; Beg, M.; Sharma, S.; Choubey, A.K., Application of manganese oxide nanoparticles synthesized via green route for improved performance of water-based drilling fluids, Applied Nanoscience, 2021, 11, 2247-2260. <https://doi.org/10.1007/s13204-021-01956-8>
  34. Henry, J.; Mohanraj, K.; Kannan, S.; Barathan, S.; Sivakumar, G., Effect of butanol and propylene glycol in amorphous MnO<sub>2</sub> nanoparticles, Walailak Journal of Science and Technology, 2014, 11(5), 437-443.
  35. Sivakumar, S.; & Prabu, L.N., Synthesis and Characterization of α-MnO<sub>2</sub> nanoparticles for Supercapacitor application, Materials Today: Proceedings, 2021, 47, 52-55. <https://doi.org/10.1016/j.matpr.2021.03.528>
  36. Sinha, A.; Singh, V.N.; Mehta, B.R.; & Khare, S.K., Synthesis and characterization of monodispersed orthorhombic manganese oxide nanoparticles produced by Bacillus sp. cells simultaneous to its bioremediation, Journal of hazardous materials, 2011, 192(2), 620-627. <https://doi.org/10.1016/j.jhazmat.2011.05.103>
  37. Hemlatha, F.C.; & Lourduraj, A.J.C., Synthesis and characterization of MnO<sub>2</sub> Nanoparticles using Co-precipitation Technique, International Journal of Scientific Research in Science and Technology, 2017, 3(11), 125-128.
  38. Akbari, S.; Mehdi, M.; & Foroughi, M., Solvent-free synthesis and characterization of MnO<sub>2</sub> nanostructures and investigation of optical properties, Journal of Nanomedicine and Nanotechnology, 2018, 9(3), 498, 1-5. <https://doi.org/10.4172/2157-7439.1000498>
  39. Du, T.; Chen, S.; Zhang, J.; Li, T.; Li, P.; Liu, J.; & Wang, S., Antibacterial activity of manganese dioxide nanosheets by ROS-mediated pathways and destroying



- membrane integrity, *Nanomaterials*, 2020, 10(8), 1-14. <https://doi.org/10.3390/nano10081545>
40. Soldatova, A. V.; Balakrishnan, G.; Oyerinde, O. F.; Romano, C. A.; Tebo, B. M.; & Spiro, T. G., Biogenic and synthetic MnO<sub>2</sub> nanoparticles: size and growth probed with absorption and Raman spectroscopies and dynamic light scattering, *Environmental science & technology*, 2019, 53(8), 4185-4197. <https://doi.org/10.1021/acs.est.8b05806>
41. Veena, M. A.; Kumar, C. H.; Majani, S. S.; Munirajappa, N. N.; Harendra, B.; Shivamallu, C.; & Kollur, S. P., Eco-friendly synthesized manganese dioxide nanoparticles using *Tridax procumbens* as potent antimicrobial and dye degrading agent, *Results in Chemistry*, 2024, 7, 101290. <https://doi.org/10.1016/j.rechem.2023.101290>